

Endurance improvement of resistance switching behaviors in the $\text{La}_{0.7}\text{Ca}_{0.3}\text{MnO}_3$ film based devices with Ag–Al alloy top electrodes

R. Yang,^{1,a)} X. M. Li,^{1,b)} W. D. Yu,¹ X. D. Gao,¹ D. S. Shang,² and L. D. Chen¹

¹State Key Laboratory of High Performance Ceramics and Superfine Microstructures, Shanghai Institute of Ceramics, Chinese Academy of Sciences, Shanghai 200050, People's Republic of China

²Beijing National Laboratory for Condensed Matter Physics and Institute of Physics, Chinese Academy of Sciences, Beijing 100190, People's Republic of China

(Received 30 September 2009; accepted 9 January 2010; published online 16 March 2010)

The resistance switching characteristics of the $\text{La}_{0.7}\text{Ca}_{0.3}\text{MnO}_3$ -based devices with the top electrodes of Ag, Ag–Al alloys with the atomic ratios of Ag:Al=2:1 (2AgAl) and Ag:Al=1:2 (Ag2Al), and Al have been investigated. The device with 2AgAl top electrode shows excellent endurance, where more than 1000 cycles of reproducible current-voltage hysteresis with stable high and low resistance states have been observed. Based on Auger electron spectroscopy measurement and the detailed investigation of current-voltage curves of these devices, it is suggested that the oxygen affinity of the metal electrode, which is determined by the chemical component of Ag and Al, has an important influence on the interface structure and the resistance switching endurance. The present work provides a possible way for the improvement of the resistance switching endurance by modulating oxygen affinity of the electrode. © 2010 American Institute of Physics. [doi:10.1063/1.3309473]

I. INTRODUCTION

The electric-pulse-induced resistance switching phenomenon in recent years has been intensively studied for its potential application to resistance random access memory (RRAM), which is a competitive candidate for the next generation nonvolatile memory (NVM).^{1,2} Comparing with other NVMs, RRAM is attractive for today's semiconductor technology due to its simple sandwich structure, high writing/erasing speed, high storage density, and low power consumption.^{3–7} Numerous transition metal oxide materials, sandwiched between the top electrode (TE) and bottom electrode (BE), have been found to exhibit resistance switching properties, such as $\text{Pr}_{0.7}\text{Ca}_{0.3}\text{MnO}_3$ (PCMO),^{2,3,6,7} $\text{La}_{0.7}\text{Ca}_{0.3}\text{MnO}_3$ (LCMO),⁸ SrTiO_3 ,^{4,5} NiO ,^{9,10} etc. Various models have been proposed in the past decade to explain the resistance switching behaviors, including trap controlled space-charge-limited conduction,^{6,8} charge trapping induced alteration of Schottky-like barrier,^{11,12} electrochemical migration of oxygen,^{4,10,13} and oxidation/reduction reaction.^{9,14–19} Even though the exact microscopic mechanism is still debated due to the lack of solid experimental evidences, there forms a general agreement that the resistance switching process mainly occurs at the TE/oxide interface. The migration of oxygen ions (vacancies) or the resultant redox reaction occurring at the TE/oxide interface has been proposed to explain the resistance switching behaviors by many researchers.^{13–21}

Apart from a further elucidation of the resistance switching mechanism, it is also considerably important to improve the endurance of the resistance switching devices for the potential application of RRAM materials.^{1,14} It has been re-

ported that the oxygen affinity of the electrode can directly influence the resistance switching endurance by adjusting the TE/oxides interface structure.^{10,20–23} Shen *et al.* reported that the resistance switching endurance of barium strontium titanate (BST) films can be effectively improved by using W instead of Pt as TE. It is suggested that the WO_x layer formed at the W/BST interface effectively blocks oxygen diffusion into the atmosphere, resulting in the endurance improvement.¹⁴ Endurance enhancement of Cu-oxide based resistive switching devices has been achieved by using Al as TE. The observed AlO_x layer at the Al/ Cu_xO interface is proposed to contribute to the endurance enhancement by blocking the oxygen diffusion between the Cu_xO film and atmosphere.²¹ Similar phenomena were also observed in MnO_2 and ZrO_2 films with Ti electrodes.^{22,23} For the complex manganite film such as LCMO or PCMO, an oxidation layer of the TE has been observed at the TE/manganite interface for the active metals such as Al, Ti, and Sm.^{16–19} In this instance, the devices usually show high yield but low speed, high threshold voltage, and inferior endurance. In special, for the endurance, the devices usually break down after tens of continuous voltage sweeping cycles. In contrast, when the noble metal such as Pt, Ag, or Cu is chosen as TE, the TE oxidation layer has not been observed at the TE/manganite interface, and the device usually shows high switching speed but low yield and is also fatigable too.^{2,6,24} Therefore, it is necessary for both the noble and active metal electrode layered devices to modulate the interface structures of TE/manganite to improve the resistance switching endurance.

Based on the above investigations, in this paper, we designed and prepared a series of novel Ag–Al alloy electrodes with different components on the LCMO film to adjust the interface structure, including pure Ag, 2AgAl with Ag:Al=2:1, Ag2Al with Ag:Al=1:2, and pure Al. The continuous voltage sweeping was systematically performed to describe

^{a)}Also at Graduate School of Chinese Academy of Sciences, Beijing 100039, People's Republic of China.

^{b)}Author to whom correspondence should be addressed. Electronic mail: lixm@mail.sic.ac.cn.

the resistance switching endurance. It is found that the Ag–Al/LCMO/Pt device shows excellent reproducible current-voltage hysteresis and resistance switching properties when the atomic ratio of Ag:Al is 2:1. Moreover the mechanism of the endurance improvement is discussed.

II. EXPERIMENT

The LCMO films of 200 nm thick were deposited on the Pt/Ti/SiO₂/Si substrates by the pulse laser deposition system. It was carried out using a Lambda Physik KrF excimer laser system (COMPex201) with the wavelength of 248 nm running with a repetition rate of 5 Hz. The oxygen partial pressure and substrate temperature during deposition were maintained at 1.5 Pa and 650 °C, respectively. The obtained film is smooth and polycrystalline, as reported elsewhere.¹⁵ Pure Ag and Al electrodes were prepared by thermal evaporation and electron beam evaporation, respectively. The Ag–Al alloy electrodes were obtained by synchronously evaporating Ag and Al. The Ag/Al ratio can be accurately adjusted by controlling the evaporating rates of Ag and Al. Two alloy electrodes of 2AgAl with nominal atomic ratios of Ag:Al=2:1 and Ag2Al with that of Ag:Al=1:2 have been prepared. The lift-off process was used to form the contact pads with diameter of 50 μm. All the electrodes are 10 nm thick and prepared at room temperature. The 50-nm-thick Pt cover layers were subsequently deposited on the electrodes by electron beam evaporation. The chemical composition of the 2AgAl/LCMO interface was examined by the Auger electron spectroscopy (AES). All the current-voltage (*I-V*) characteristics and electric-pulse-induced resistance switching behaviors were carried out with the standard two-wire method at room temperature. A positive bias is defined as the current flows into the manganite film through TE and out from BE. Unless specified, the *I-V* characteristics were measured by voltage sweeping as $0 \rightarrow +V_{\max} \rightarrow 0 \rightarrow -V_{\max} \rightarrow 0$ with voltage step of 0.02 V. The sweeping time for each step was fixed at 0.25 s.

III. RESULTS AND DISCUSSION

The continuous *I-V* curves are usually used to characterize the resistance switching endurance of the devices.^{14,22,25} Figure 1 shows the typical continuous *I-V* curves of the TE/LCMO/Pt devices with various TEs of pure Ag, 2AgAl, Ag2Al, and pure Al. For the Ag/LCMO/Pt device, as shown in Fig. 1(a), the first 50 cycles show hysteresis indicating the resistance decreases (increases) by applying positive (negative) bias, which is defined as the negative bipolar resistance switching (BRS) behaviors.¹⁵ However the hysteresis window disappears when the number of the voltage sweeping cycles increases up to 100. That is to say this device is fatigued after 100 cycles of resistance switching. To clarify the fatigued phenomenon, the resistances of high resistance state (HRS) and low resistance state (LRS) during the voltage sweeping process (read at 0.1 V) are shown in the inset of Fig. 1(a). From this inset, we can see that the resistance value of the device keeps at LRS after about 90 cycles of voltage sweeping. Ten original devices had been measured and all of them were fatigued after 100 cycles of voltage sweeping al-

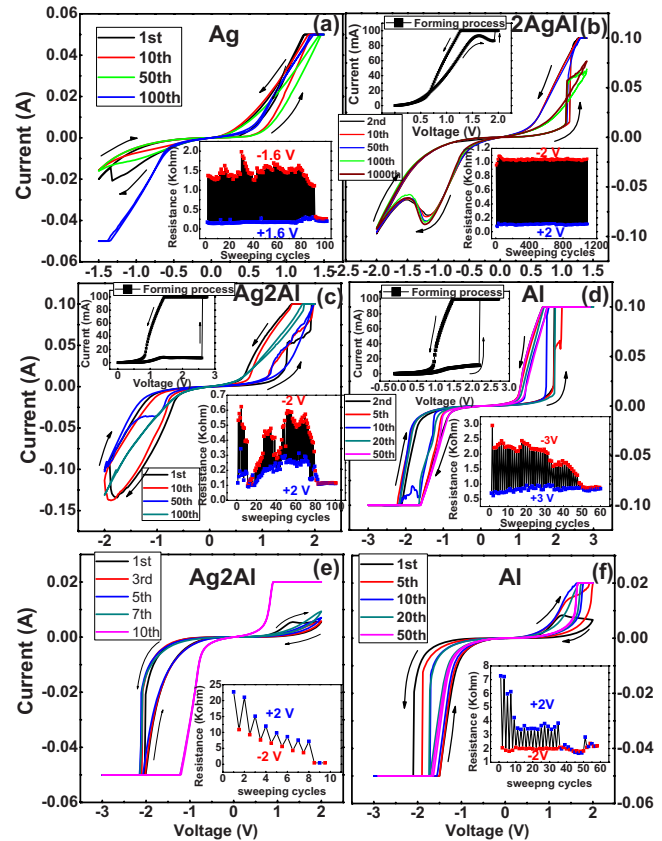


FIG. 1. (Color online) The continuous *I-V* curves of TE/LCMO/Pt devices for TE is pure Ag (a), 2AgAl (b), Ag2Al [(c) and (e)], and pure Al [(d) and (f)]. The lower insets show the resistances of HRS and LRS (read at 0.1 V) during the voltage sweeping process. The upper insets of (b)–(d) show the forming processes.

though the resistance evolutions during the voltage sweeping process showed some differences between each other. It should be mentioned that the adhesion strength between Ag electrode and LCMO film is relatively low. The Ag electrodes were usually destroyed by the scratching of the measuring probe. The adhesion strength between them can be improved by heating the LCMO film up to 200 °C during the preparation process of Ag electrodes. However, in this instance, the devices show almost Ohmic behavior and no hysteresis in the *I-V* curves, which is consistent with the previous reports.^{26–28} However, the adhesive strength of the electrode can be effectively improved when some Al is added to Ag electrode to form the Ag–Al alloy electrode.

In contrast to the Ag layered device, the 2AgAl layered device shows excellent endurance, as shown in Fig. 1(b). The upper inset of Fig. 1(b) replots the first *I-V* curve at the positive bias region. From this figure, we can see that an obvious negative differential resistance (NDR) effect appears at about 1.6 V. Then, a soft breakdown occurs when the sweeping voltage increases up to about 1.9 V. A current compliance of 100 mA is applied to protect the sample. This process is defined as the forming process because the stable and reproducible *I-V* curves can only be obtained after this process. After the forming process, the current abruptly increases at about 1.0 V, resulting in LRS. In the negative bias region, when the voltage reaches about –1.2 V, a NDR effect occurs, resulting in HRS. It can be seen that the 2AgAl lay-

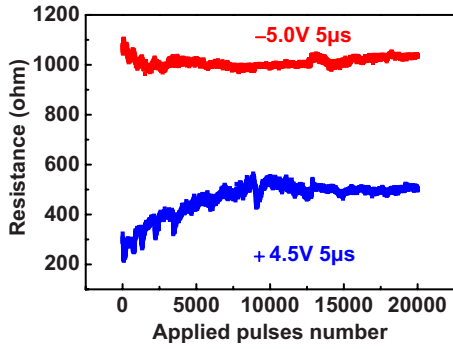


FIG. 2. (Color online) Resistance switching behavior of the 2AgAl/LCMO/Pt device induced by applying electric pulses of 4.5/−5.0 V with pulse duration of 5 μ s.

ered device shows the same switching polarity as the Ag layered device. However, the 2AgAl layered device shows much better endurance than the Ag layered device. As shown in Fig. 1(b), the I - V curve of the 100th cycle still shows big hysteresis comparing with that of the 2nd cycle, although a shrink happens in the positive bias. No more shrink has been observed in the following I - V curves. Moreover the I - V curve of the 1000th cycle is almost the same as that of the 100th cycle. The lower inset of Fig. 1(b) shows the resistances of HRS and LRS (read at 0.1 V) during the voltage sweeping process. From this inset, we can see that the resistance values of HRS and LRS are very stable except a little fluctuation occurs in the first 100 cycles, which indicates the endurance improvement of the devices by alloying Al into the pure Ag electrode.

The other two kinds of devices with electrodes of Ag2Al and pure Al have also been studied to investigate the influence of the Ag–Al alloy component on the resistance behaviors, as shown in Figs. 1(c) and 1(d), respectively. The similar forming processes have been applied, as shown in the upper insets of Figs. 1(c) and 1(d). After the forming processes, both devices also show the negative BRS with inferior endurance. The resistance values of HRS and LRS (read at 0.1 V) during the voltage sweeping process replotted in the lower insets of Figs. 1(c) and 1(d) clearly show the instability and fatigue of the resistance switching behavior. It should be noted that the pure Al layered device naturally shows the positive BRS without the forming process, in which the resistance increases (decreases) by applying positive (negative) bias, as shown in Fig. 1(f). The polarity reversal can be ascribed to the structure changes occurring at the Al/LCMO interface during the forming process.²⁹ As shown in Fig. 1(e), the Ag2Al layered device also shows positive BRS without the forming process, which is similar to the pure Al layered device. From Figs. 1(e) and 1(f), we can see that the positive BRS behaviors are also fatigable in both the pure Al and Ag2Al layered devices. Based on the above results, it can be seen that the component of TEs has an important influence on the resistance switching properties, and the 2AgAl layered device shows the excellent endurance.

The electric-pulse-induced resistance switching behavior of the 2AgAl/LCMO/Pt device has been performed to test the endurance. As shown in Fig. 2, an endurance of over 2

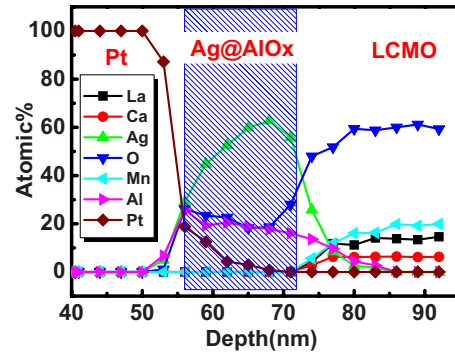


FIG. 3. (Color online) The AES depth profile of the original 2AgAl/LCMO interface structure.

$\times 10^4$ cycles with the resistance switching ratio $[(R_{\text{HRS}} - R_{\text{LRS}})/R_{\text{LRS}}]$, R_{HRS} , and R_{LRS} indicate the resistance values of HRS and LRS, respectively] larger than 100% was obtained. The applied pulse voltages were 4.5 and −5 V with pulse duration of 5 μ s for the resistance decrease and increase, respectively. The fatigued phenomenon only happens in the first 10^4 cycles, after which the resistances of HRS and LRS become stable and show an excellent endurance. It is expected that the stability of the resistance switching would be further improved by adjusting the conditions of the applied pulses. Besides the endurance improvement, the adhesive strength of the electrodes and the yield of the devices have also been improved by using Ag–Al alloy electrodes, which means that the alloy electrode has promising potential application in RRAM devices.²⁶

In order to investigate the mechanism of the endurance improvement, the original structure of the 2AgAl/LCMO interface has been examined by AES depth profile analysis. As shown in Fig. 3, the percentage of oxygen at the Ag–Al region is about 20%, indicating that the alloy electrode was oxidized. Figures 4(a) and 4(c) show the AES spectra of Ag and Al elements in the 2AgAl electrode. For comparison, the standard AES spectra of metallic Ag, metallic Al, and oxidized Al in the $\text{AlO}_{1.17}$ oxides are also shown in Figs. 4(b) and 4(d), respectively. The AES spectra of Ag in the 2AgAl alloy are almost the same as that of metallic Ag, indicating that Ag was not oxidized. In contrast, the AES spectra of Al in the 2AgAl alloy are different from the metallic Al but similar to that of the $\text{AlO}_{1.17}$ oxide, indicating that Al was oxidized in the 2AgAl alloy electrode. That is to say, the 2AgAl alloy is a composite structure containing Ag and AlO_x . These results are consistent with our previous studies, in which the Al electrode with 10 nm thickness can be completely oxidized to form an AlO_x layer, while the TE oxidation layer has not been observed at the Ag/LCMO interface.^{18,29} Based on above results, we can see that the AlO_x content at the TE/LCMO interface determined by the alloy electrode component has an important influence on the resistance switching endurance.

Compared to the Ag layered device, the added forming process in the 2AgAl layered device may contribute to the endurance improvement. So, the forming process is investigated in detail. Figure 5 shows the I - V curves measured between a fixed negative bias of −2 V and a gradually increas-

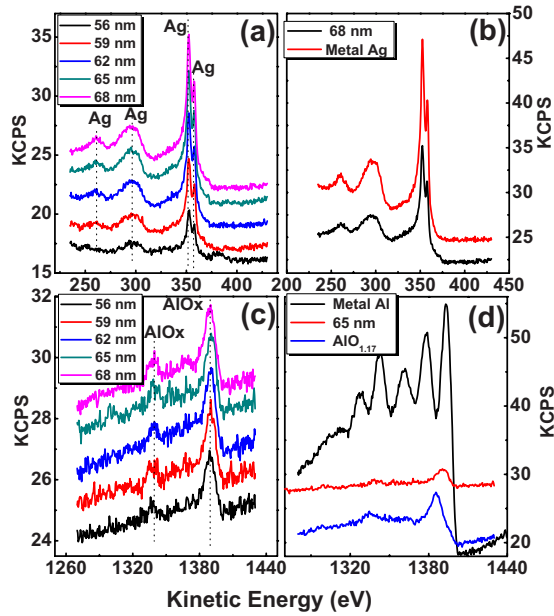


FIG. 4. (Color online) The AES spectra of Ag (a) and Al (c) elements in the 2AgAl alloy electrode, the AES spectra of the metallic Ag and Ag element in the 2AgAl electrode at depth of 68 nm (b), the AES spectra of the metallic Al, Al in the 2AgAl alloy electrode at depth of 65 nm, and the oxidized Al in $\text{AlO}_{1.17}$ (d).

ing positive bias from 0 to 2 V. As shown in Fig. 5(a), the hysteresis has not been observed in either the positive or negative bias regions until the positive bias reaches 1.7 V (the fifth cycle). Then an obvious clockwise hysteresis appears in the positive bias region, indicating the device resistance increases. This process should be related to the oxidation reaction of AlO_x at the 2AgAl/LCMO interface.^{16,29} At the sixth cycle, a soft-broken process occurs when the positive bias increases up to about 1.9 V, then big hysteresis windows appear in both the positive and negative bias regions, seen the seventh and eighth cycles in Fig. 5. The soft-broken process might be related to the formation of Ag filaments in the alloy electrode. Afterward, the point contact structure of Ag might form at the 2AgAl/LCMO interface and results in the stable resistance switching property, which is analogous to the Ag paste layered device.^{6,28}

At the TE/oxides interface, the oxygen affinity of the electrode has important influences on the interface structure

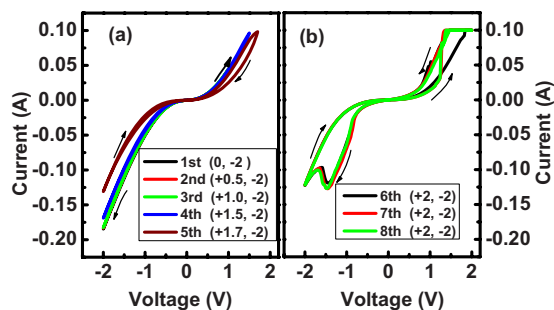


FIG. 5. (Color online) The I - V curves of the 2AgAl/LCMO/Pt device with the fixed negative bias of -2 V and gradually increasing positive bias from 0 to 2 V. The first, second, third, fourth, and fifth cycles with positive biases of 0, 0.5, 1.0, 1.5, and 1.7 V, respectively (a). The sixth to the eighth cycles with the positive bias of 2 V (b).

and the resistance switching properties.^{21–23,30} For the inert TE, such as Pt and Ag, oxygen can diffuse along the grain boundaries.³¹ So the atmospheric oxygen could diffuse into the interface region and influence the oxygen migration balance occurring during the resistance switching process.^{21–23} This may be the underlying reason for the fatigue phenomenon depicted in Fig. 1(a). In contrast, for the active TE, the formed metal oxidation layer at the interface could reduce the influence of the atmospheric oxygen. However, in LCMO based devices, it has been reported that very active metals degrade the switching speed and endurance.³⁰ Our results also show that very active metals result in an inferior endurance, as shown in Figs. 1(c)–1(f). Therefore, some compromise needs to be made to modulate the oxygen affinity of the electrode. For the Ag–Al alloy electrodes, the oxygen affinity can be modulated by adjusting the ratio of the Al and Ag elements. The 2AgAl electrode may have the proper oxygen affinity and forms a composite structure containing Ag and AlO_x at the interface. In this instance, Ag plays the dominating role and the proper amount of AlO_x may block the oxygen diffusion between the atmosphere and the LCMO film, which results in excellent endurance. However, if the proportion of Al is in excess of Ag or pure Al is used as TE, the AlO_x could form a continuous layer and dominate the resistance switching process. In this instance, it has been verified that the redox reaction of the AlO_x layer determines the positive BRS.^{15,17} In positive BRS process, the devices usually break down after a few sweeping cycles due to the randomness of the redox reaction position and the needed high threshold voltage. So, the Ag2Al and pure Al layered devices show the positive BRS with inferior stability and endurance, as shown in Figs. 1(e) and 1(f). By applying the forming process, these devices can show negative BRS, but fatigue usually occurs too. This may be because the formed conductive filaments are instable due to the insufficient of Ag in AlO_x matrix. Our experimental results indicate that the control over the oxygen affinity of the electrode is critical to obtain preferable endurance. Further investigations on the Ag–Al alloy interface structure and studies on the function of the oxygen ions (vacancies) during the resistance switching process have been launched to understand the endurance improvement mechanism.

IV. CONCLUSION

In order to improve the endurance of the LCMO film based resistance switching devices, the novel Ag–Al alloy electrodes with various components have been prepared. Compared to the devices with pure Ag, Ag2Al, and pure Al TEs, the 2AgAl layered device shows the excellent endurance. More than 1000 cycles of voltage sweeping with very stable HRS and LRS have been observed. By applying the electric pulses of 4.5/–5 V for 5 μs , an endurance of over 2×10^4 cycles with the resistance switching ratio about 100% has been obtained. The AES measurement indicates that the 2AgAl TE has a composite structure containing Ag and AlO_x . The endurance improvement was attributed to the proper ratio of AlO_x at the 2AgAl/LCMO interface. The

present work suggests a possible way to improve the resistance switching endurance by modulating oxygen affinity of the electrode.

ACKNOWLEDGMENTS

This work was sponsored by the 973 National Nature Science Foundation (Grant No. 2009CB623304), the Key-stone Project of Shanghai Basic Research Program (Grant No. 08JC1420600), the Shanghai-AM Research and Development Fund (Grant No. 8700740900), and the Nature Science Foundation of Shanghai (Grant No. 08ZR1421500).

- ¹G. I. Meijer, *Science* **319**, 1625 (2008).
- ²S. Q. Liu, N. J. Wu, and A. Ignatiev, *Appl. Phys. Lett.* **76**, 2749 (2000).
- ³R. Waser, R. Dittmann, G. Staikov, and K. Szot, *Adv. Mater. (Weinheim, Ger.)* **21**, 2632 (2009).
- ⁴K. Szot, W. Speier, G. Bihlmayer, and R. Waser, *Nature Mater.* **5**, 312 (2006).
- ⁵K. Szot, R. Dittmann, W. Speier, and R. Waser, *Phys. Status Solidi (RRL)* **1**, R86 (2007).
- ⁶M. Fujimoto, H. Koyama, Y. Nishi, and T. Suzuki, *Appl. Phys. Lett.* **91**, 223504 (2007).
- ⁷S. L. Li, J. L. Gang, J. Li, H. F. Chu, and D. N. Zheng, *J. Phys. D: Appl. Phys.* **41**, 185409 (2008).
- ⁸D. S. Shang, Q. Wang, L. D. Chen, R. Dong, X. M. Li, and W. Q. Zhang, *Phys. Rev. B* **73**, 245427 (2006).
- ⁹C. B. Lee, B. S. Kang, A. Benayad, M. J. Lee, S. E. Ahn, K. H. Kim, G. Stefanovich, Y. Park, and I. K. Yoo, *Appl. Phys. Lett.* **93**, 042115 (2008).
- ¹⁰C. Yoshida, K. Kinoshita, T. Yamasaki, and Y. Sugiyama, *Appl. Phys. Lett.* **93**, 042106 (2008).
- ¹¹A. Sawa, T. Fujii, M. Kawasaki, and Y. Tokura, *Appl. Phys. Lett.* **85**, 4073 (2004).
- ¹²J. J. Yang, M. D. Pickett, X. M. Li, D. A. A. Ohlberg, D. R. Stewart, and R. S. Williams, *Nat. Nanotechnol.* **3**, 429 (2008).
- ¹³Y. B. Nian, J. Strozier, N. J. Wu, X. Chen, and A. Ignatiev, *Phys. Rev. Lett.* **98**, 146403 (2007).
- ¹⁴W. Shen, R. Dittmann, U. Breuer, and R. Waser, *Appl. Phys. Lett.* **93**, 222102 (2008).
- ¹⁵R. Yang, X. M. Li, W. D. Yu, X. D. Gao, D. S. Shang, X. J. Liu, X. Cao, Q. Wang, and L. D. Chen, *Appl. Phys. Lett.* **95**, 072105 (2009).
- ¹⁶K. Shono, H. Kawano, T. Yokota, and M. Gomi, *Appl. Phys. Express* **1**, 055002 (2008).
- ¹⁷S.-L. Li, D. S. Shang, J. Li, J. L. Gang, and D. N. Zheng, *J. Appl. Phys.* **105**, 033710 (2009).
- ¹⁸M. Hasan, R. Dong, H. J. Choi, D. S. Lee, D. J. Seong, M. B. Pyun, and H. Hwang, *Appl. Phys. Lett.* **92**, 202102 (2008).
- ¹⁹H. Kawano, K. Shono, T. Yokota, and M. Gomi, *Appl. Phys. Express* **1**, 101901 (2008).
- ²⁰J. Joshua Yang, F. Miao, M. D. Pickett, D. A. A. Ohlberg, D. R. Stewart, C. N. Lau, and R. Stanley Williams, *Nanotechnology* **20**, 215201 (2009).
- ²¹H. B. Lv, M. Wang, H. J. Wan, Y. L. Song, W. J. Luo, P. Zhou, T. G. Tang, Y. Y. Lin, R. Huang, S. Song, J. G. Wu, H. M. Wu, and M. H. Chi, *Appl. Phys. Lett.* **94**, 213502 (2009).
- ²²M. K. Yang, J. W. Park, T. K. Ko, and J. K. Lee, *Appl. Phys. Lett.* **95**, 042105 (2009).
- ²³C. Y. Lin, C. Y. Wu, T. Y. Tseng, and C. M. Hu, *J. Appl. Phys.* **102**, 094101 (2007).
- ²⁴D. S. Shang, L. D. Chen, Q. Wang, Z. H. Wu, W. Q. Zhang, and X. M. Li, *J. Phys. D: Appl. Phys.* **40**, 5373 (2007).
- ²⁵R. Dong, W. F. Xiang, D. S. Lee, S. J. Oh, D. J. Seong, S. H. Heo, H. J. Choi, M. J. Kwon, M. Chang, M. Jo, M. Hasan, and H. S. Hwang, *Appl. Phys. Lett.* **90**, 182118 (2007).
- ²⁶W. D. Yu, X. M. Li, Y. Rui, X. J. Liu, Q. Wang, and L. D. Chen, *J. Phys. D: Appl. Phys.* **41**, 215409 (2008).
- ²⁷R. Yang, X. M. Li, W. D. Yu, X. J. Liu, X. D. Gao, Q. Wang, and L. D. Chen, *Appl. Phys. A: Mater. Sci. Process.* **97**, 85 (2009).
- ²⁸C. Jooss, J. Hoffmann, J. Fladerer, M. Ehrhardt, T. Beetz, L. Wu, and Y. Zhu, *Phys. Rev. B* **77**, 132409 (2008).
- ²⁹R. Yang, X. M. Li, W. D. Yu, X. J. Liu, X. Cao, Q. Wang, and L. D. Chen, *Electrochem. Solid-State Lett.* **12**, H281 (2009).
- ³⁰M. Hasan, R. Dong, H. Choi, J. Yoon, J. B. Park, D. J. Seong, and H. Hwang, *J. Electrochem. Soc.* **156**, H239 (2009).
- ³¹R. Schmiel, V. Demuth, P. Lahnor, H. Godehardt, Y. Bodschiwinna, C. Harder, L. Hammer, H. P. Strunk, M. Schulz, and K. Heinz, *Appl. Phys. A: Mater. Sci. Process.* **62**, 223 (1996).